

Quiet & Stormtime Production & Loss Rates: Smith's Technique

N S CHAUHAN & H S GURM

Department of Astronomy & Space Sciences, Punjabi University, Patiala 147002

Received 13 August 1984; revised received 28 November 1984

The monthly values of production and loss rate have been inferred by fitting the computed and observed total electron contents (TEC) from ATS-6 transmissions at six closely spaced low-latitude stations. A sunrise model of the low-latitude ionosphere is constructed by solving the plasma continuity equation. Comparison between the computed and the observed values of TEC yields the best fit average production rate of atomic oxygen at sunrise as $1.26 \times 10^{13} \text{ m}^{-2} \text{ sec}^{-1}$ and average loss coefficient at 300 km as $1.13 \times 10^{-5} \text{ sec}^{-1}$. The production rates for all the stations show semi-annual variations with maxima in equinoxes and minima in solstices. Latitudinally, it exhibits an increasing trend in its values towards the equator. The summer-to-winter ratio in loss coefficient is 1:2 at Patiala and it diminishes towards the equator. The stormtime production rate is found to exceed the quiettime value.

1 Introduction

The rate of production of electrons in the F-region is due to the photoionization of atmospheric constituents. At sunrise, the rate of increase of the ionospheric electron content (IEC) is essentially equal to the height integral of production rate¹⁻². The loss of electrons in the ionosphere is negligible at ground level during sunrise, primarily, because the electron concentration itself is small and, secondly, because a large part of production at sunrise occurs at altitudes where the loss coefficient is small. After sunrise, the loss rate of electrons integrated with respect to height through the ionosphere rapidly approaches the height-integrated production rate, thus limiting the rate of change of electron content. Knowing a detailed time behaviour of the electron content during a period near the sunrise, it is possible to find out both the height-integrated production rate at the sunrise and F2-region loss rate coefficient.

Several workers¹⁻¹⁰ have calculated the production and loss rates. They have used the familiar graphical curve-fitting technique to get the value of production rates. A sophisticated technique based on fitting the observed and computed TEC was developed by Smith¹¹ for the calculation of production and loss rates. This technique has the advantage of taking care of transport of ionization in the calculation of production rate; and, also the loss rate is evaluated along with the production rate. The present study involves the computation of production and loss rates, during quiet and disturbed periods using Smith's method.

2 Computation

The total electron content (TEC) data from the geostationary satellite, ATS-6, for the period Oct.

1975-July 1976 are used for the present analysis. The transmission from ATS-6 was received simultaneously at six low-latitude stations [Patiala (lat., 30.32°N; long., 76.38°E), Udaipur (lat., 24.58°N; long., 73.67°E), Ahmedabad (lat., 23.03°N; long., 72.62°E), Rajkot (lat., 22.31°N; long., 70.74°E), Bombay (lat., 19.09°N; long., 72.91°E) and Thumba (lat., 8.55°N; long., 76.89°E)] over the Indian zone. Out of six stations the data from Rajkot and Thumba are available only for the period Dec. 1975-June 1976 and Nov. 1975-July 1976, respectively. Further, the proximity of the six stations in the present study provides an opportunity to know about the latitudinal production rate profile and a possible mechanism explaining their differences.

The sunrise model of the low-latitude ionosphere is constructed by solving the following plasma continuity equation¹².

$$\frac{\partial N}{\partial t} = q - L - \nabla \cdot (NW_1) - \nabla \cdot (NW_2) - \nabla \cdot (NW_3) \quad \dots (1)$$

where

- q Production rate
- N Electron density
- L Linear loss rate given by

$$L = \beta N = \beta_{300} \exp[-1.75z] \quad \dots (2)$$

where

- z Reduced height = $(h - 300)/H$
- h Height above the surface of the earth
- H Scale height of atomic oxygen

The last three divergence terms of Eq. (1) account for the contribution due to $\mathbf{E} \times \mathbf{B}$ drift, ambipolar diffusion and neutral wind, respectively.

To calculate the loss coefficient, β_{300} , at 300 km and sunrise production rate $Q_{90}(\text{O}^+)$, Eq. (1) is solved for a

given initial value of both β_{300} and $Q_{90}(O^+)$ during the sunrise period ($100^\circ \geq \chi \geq 87^\circ$). The computed values of the integrated electron density are compared with experimentally observed TEC values to get the best fitted values of β_{300} and $Q_{90}(O^+)$. The general scheme of calculation is presented by Smith in Fig. 1 of his work¹¹. The overhead production rate is deduced from $Q_{90}(O^+)$ through the relation

$$Q_0(O^+) = Q_{90}(O^+) \cdot \text{Chap}(\chi, H) \quad \dots(3)$$

where $\text{Chap}(\chi, H)$ is the Chapman function.

3 Results

3.1 Production Rate

In Fig. 1 all the stations show semi-annual variations with higher value of production rate in equinoxes compared to those in solstices. The station, Thumba, closest to the equator, shows weak semi-annual variations. At other stations, the semi-annual variations are of comparable magnitude. These semi-annual variations could be due to the variations in O/N_2 ratio as reported by Mayr and Mahajan¹³. Similar variations in TEC have also been reported by Iyer¹⁴. It is noticed that the winter values of production rate for all the stations except Thumba are more than the summer values (Table 1). This is in conformity with the occurrence of well-known seasonal anomaly¹⁵. However, the average value of $Q_{90}(O^+)$ for all the stations and for all the months comes out to be $1.26 \times 10^{13} \text{ m}^{-2} \text{ sec}^{-1}$. Using relation (3), the mean value of overhead production rate $Q_0(O^+)$ for all the stations

and for all the months comes out to be $1.13 \times 10^{14} \text{ m}^{-2} \text{ sec}^{-1}$. The present value agrees with the values obtained by Taylor³, Walker¹⁶, Deshpande *et al.*⁸ and Singh *et al.*¹⁰.

Fig. 2 depicts the latitudinal variation of the production rate. The production rate shows generally an increasing trend as the equator is approached from higher latitudes. This agrees with the production rates obtained from the computation of standard model atmosphere of Jacchia¹⁷. At Thumba, a station closest to the equator, the production rate for all the seasons is of comparable magnitude and it is significantly greater than the average value of $1.26 \times 10^{13} \text{ m}^{-2} \text{ sec}^{-1}$. The equinoxial values of the production rate for all the stations are greater than those for other seasons.

3.2 Loss Rate

The value of linear loss coefficient, β_{300} , at 300 km for which the root mean square difference is minimum, is found out for all the stations and for all the months (Table 2). The average value of β_{300} for all the stations comes out to be $1.13 \times 10^{-5} \text{ sec}^{-1}$. It is noticed that the winter values of β_{300} are more than the summer values for all the stations. At Patiala, the summer-to-winter ratio is 1:2 and this decreases towards the equatorial station (Table 2). Titheridge² obtained a mean loss rate at sunset to be about $1.4 \times 10^{-5} \text{ sec}^{-1}$ in winter; and this value decreased to $0.5 \times 10^{-5} \text{ sec}^{-1}$ in summer. Prasad¹⁸, using data from Arecibo, Puerto Rico, found β_{300} to be $1.07 \times 10^{-5} \text{ sec}^{-1}$, while Quinn and Nishbet¹⁹ found it to be about $2 \times 10^{-5} \text{ sec}^{-1}$ during the low solar activity period. Smith¹¹ using the same method as the one used by us found β_{300} to be $1.4 \times 10^{-5} \text{ sec}^{-1}$. The value of β_{300} presently calculated

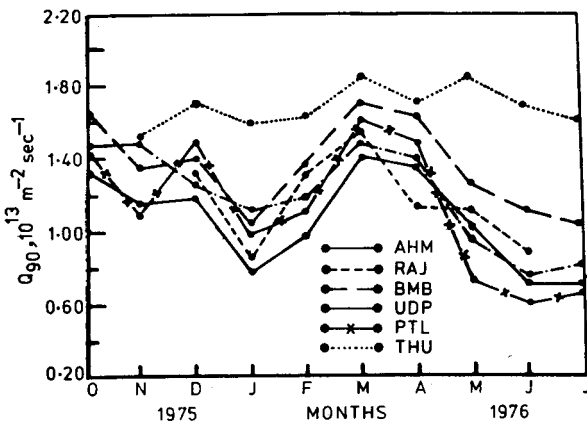


Fig. 1—Seasonal variation of $Q_{90}(O^+)$ for the period 1975-76

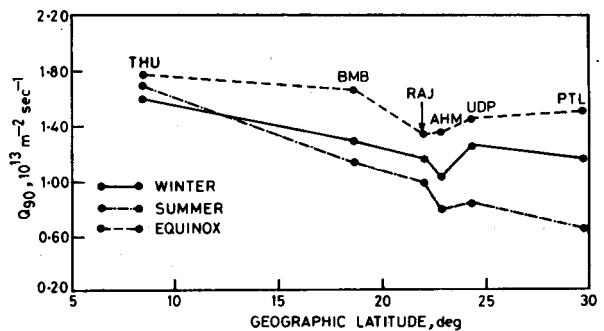


Fig. 2—Latitudinal variation of $Q_{90}(O^+)$ for the period 1975-76

Table 1—Production Rate, $Q_{90}(O^+)$, at Sunrise (in $10^{13} \text{ m}^{-2} \text{ sec}^{-1}$)

Season	Station					
	Thumba	Bombay	Rajkot	Ahmedabad	Udaipur	Patiala
Equinoxes	1.76	1.64	1.32	1.34	1.43	1.49
Winter	1.59	1.28	1.15	1.01	1.24	1.15
Summer	1.69	1.12	0.98	0.79	0.83	0.65

Table 2—Values of β_{300} (in 10^{-5}sec^{-1}) for Different Stations for Different Months

Month	Station					
	Thumba	Bombay	Rajkot	Ahmedabad	Udaipur	Patiala
Oct.	—	0.85	—	1.17	1.15	1.36
Nov.	0.98	1.05	—	1.19	1.20	1.25
Dec.	1.10	1.17	1.10	1.26	1.32	1.45
Jan.	1.16	1.30	1.35	1.38	1.44	1.61
Feb.	1.14	1.24	1.28	1.35	1.38	1.40
Mar.	1.10	1.27	1.26	1.30	1.30	1.47
Apr.	0.99	1.19	1.18	1.22	1.10	1.22
May	0.98	1.02	1.15	1.05	0.90	0.90
June	0.90	0.91	0.85	0.89	0.80	0.80
July	0.87	0.81	—	0.75	0.70	0.70

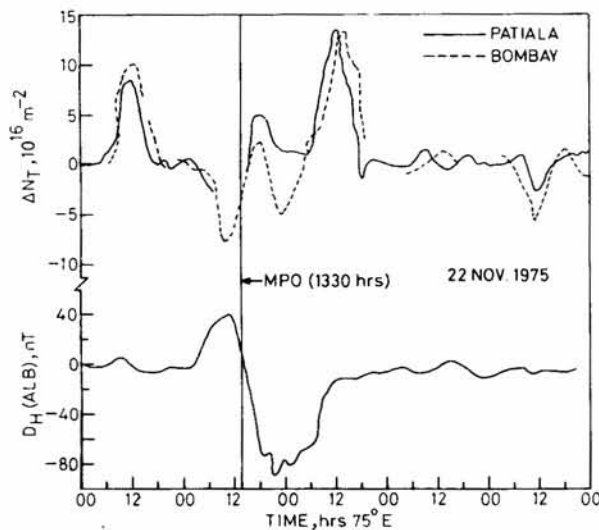


Fig. 3—Curves showing the changes in TEC and disturbed component of horizontal field at Alibag during the storm period

agrees well with the values obtained by the above workers^{11,18,19}. Calculations done during the period of high solar activity generally show higher value of loss coefficient because of increase of N_2 concentration²⁰.

4 Stormtime Production and Loss Rates

The present modelling procedure has been extended to estimate the values of production and loss rate during the disturbed conditions. We have chosen a 'great storm' commencing on 22 Nov. 1975 having main phase onset (MPO) at 1330 hrs 75°E . The range of horizontal field at Alibag, a low latitude station (geomag. lat., 9.5°), is 208 nT. The days 13-16 and 27 Nov. 1975 have been considered as quiet ones for the above storm.

Fig. 3 shows the difference between disturbed day TEC and quiet day TEC against the time of the storm for Bombay (a station on the crest of the equatorial anomaly) and Patiala (a station away from equatorial

 Table 3—Values of Production Rate (in $10^{13} \text{m}^{-2} \text{sec}^{-1}$) during 22 Nov. 1975 Storm for Bombay and Patiala

Day	Production rate for the station	
	Bombay	Patiala
21	1.3	1.4
22	1.6	1.9
23	2.2	2.6
24	1.4	1.8
25	1.2	1.35
Quiet day mean	1.2	1.3

anomaly). The TEC values for one day prior to MPO and 4 days after the MPO are plotted. The disturbed component of the horizontal field H at Alibag, $D_H(\text{ALB})$, is defined as

$$D_H(\text{ALB}) = H_D(\text{ALB}) - H_Q(\text{ALB}) \quad \dots (4)$$

where H_D and H_Q are the values of H on disturbed day and average value of H on quiet day, respectively, at Alibag.

Table 3 presents the values of production rate for different days during the storm. The average values of quiet day sunrise production rate $Q_{90}(\text{O}^+)$ for Bombay and Patiala are $1.20 \times 10^{13} \text{m}^{-2} \text{sec}^{-1}$ and $1.30 \times 10^{13} \text{m}^{-2} \text{sec}^{-1}$, respectively. On the day following MPO, i.e. 23 November the production rate increases to a maximum value of $2.2 \times 10^{13} \text{m}^{-2} \text{sec}^{-2}$ and $2.6 \times 10^{13} \text{m}^{-2} \text{sec}^{-2}$ for Bombay and Patiala, respectively. The loss rate also shows an increase in its value; but since these changes are small they are not tabulated. Fig. 3 shows that there is an increase in TEC during the first three days of the storm. Although $D_H(\text{ALB})$ after the MPO, shows sharp decrease in its value, yet the ionization near the crest of the anomaly, i.e. at Bombay, is enhanced. Normally, with the decrease of horizontal field, the pumping up of the ionization from the equator to the nearby latitudes should slow down and this should be reflected in the form of reduced TEC around the crest of the anomaly. It seems that the decrease in TEC at Bombay has been

compensated by some other process which not only makes up for the deficit of ionization but also causes an increase in total amount of ionization. Various processes such as convergence of plasma by neutral wind²¹, the plasmaspheric flux^{22,23} and circulation of neutrals^{15,24,25} can be thought of as possible explanation. At low-latitudes, the magnetic field lines do not rise very high above the equator. So the entry of plasmaspheric flux is ruled out. Neutral wind effects at these latitudes are also small as the magnitude of neutral wind itself at sunrise is small. A possible explanation, therefore, can be the increase of ionizable neutrals due to the circulation of neutrals during the disturbed conditions.

The large-scale circulation of neutrals resulting from joule dissipation during the storms induces the upwelling of air rich in molecular species over high temperature region (high latitudes) and subsequent settling of air rich in atomic oxygen over low temperature region, i.e. low-latitudes^{26,27}. This has been suggested as a mechanism responsible for the increase in atomic oxygen at the turbopause²⁸ and was confirmed by NACE experiment on AE-C by actually measuring the composition during the storms²⁹. The observations show pronounced enhancement in helium and atomic oxygen at low-latitudes.

It is thus inferred that the present increase in production rate values during the storm can be due to the increase in neutral atomic oxygen density at low-latitudes which gets transported from high latitude regions. The production rate maximizes the next day after the MPO which could be due to the fact that the atomic oxygen takes time to travel to low-latitudes. There can also be an increase in production rate due to the increase in electromagnetic radiations during the storm, but their signature should be visible soon after the storm starts. Similarly, the ionization due to corpuscular radiation is very small and is mostly confined to auroral latitudes.

References

- 1 Garriott O K & Smith F L, *Planet & Space Sci (GB)*, **13** (1965) 839.
- 2 Titheridge J E, *J Atmos & Terr Phys (GB)*, **28** (1966) 1135.
- 3 Taylor G N, *Planet & Space Sci (GB)*, **13** (1965) 507.
- 4 Tyagi T R & Mitra A P, *J Atmos & Terr Phys (GB)*, **32** (1970) 1807.
- 5 Spurling P H, *J Atmos & Terr Phys (GB)*, **34** (1972) 1151.
- 6 Titheridge J E, *J Atmos & Terr Phys (GB)*, **36** (1974) 1249.
- 7 Koster J R, *J Atmos & Terr Phys (GB)*, **38** (1974) 611.
- 8 Deshpande M R, Rastogi R G, Bhonsle R V, Sawant H S, Iyer K N, Bansidhar, Janve A V, Rai R K, Malkiat Singh, Gurm H S, Jain A R, Patwari A & Subbarao B S, *Proceedings of COSPAR Symposium on Beacon satellite held at Boston, 1976*, 268.
- 9 Majid A & Bhuriwala N V, *Ann Geophys (France)*, **32** (1976) 57.
- 10 Singh M, Salaria B S & Gurm H S, *Indian J Radio & Space Phys*, **8** (1979) 134.
- 11 Smith F L, *J Geophys Res (USA)*, **73** (1968) 7385.
- 12 Chauhan N S & Gurm H S, *Indian J Radio & Space Phys*, **9** (1980) 7.
- 13 Mayr H G & Mahajan K K, *J Geophys Res (USA)*, **76** (1971) 1017.
- 14 Iyer K N, *Studies of geomagnetism and ionosphere at low latitudes*, Ph D thesis, Gujarat University, Ahmedabad, 1976.
- 15 Chauhan N S, Gurm H S & Janve A V, *J Atmos & Terr Phys (GB)*, **42** (1980) 265.
- 16 Walker G O, *J Atmos & Terr Phys (GB)*, **33** (1971) 1041.
- 17 Jacchia L G, *Smithsonian Astrophys Obs. rep. No. 313*, Cambridge, Massachusetts, 1970.
- 18 Prasad S S, *J Atmos & Terr Phys (GB)*, **29** (1967) 987.
- 19 Quinn T P & Nishbeth J S, *J Geophys Res (USA)*, **70** (1965) 113.
- 20 Jacchia L G, *Smithson Contr Astrophys (Washington)*, **8** (1965) 215.
- 21 Ruster R & King J W, *J Atmos & Terr Phys (GB)*, **38** (1976) 596.
- 22 Mendillo M, Papagiannis M D & Klobuchar J A, *J Atmos & Terr Phys (GB)*, **31** (1969) 1359.
- 23 Mendillo M, Papagiannis M D & Klobuchar J A, *Radio Sci (USA)*, **6** (1970) 895.
- 24 Stubbe P & Chandra S, *Indian J Pure & Appl Phys*, **9** (1971) 542.
- 25 Chauhan N S & Gurm H S, *Indian J Radio & Space Phys*, **8** (1979) 106.
- 26 Rishbeth N, *J Atmos & Terr Phys (GB)*, **37** (1975) 1055.
- 27 Duncan R A, *J Atmos & Terr Phys (GB)*, **34** (1969) 59.
- 28 Obayashi T & Matuura N, *Solar Terrestrial Physics*, edited by E R Dyer (D Reidel Publishing Co), 1972, 199.
- 29 Hedin A E, Baur P, Mayr H G, Carignan G R, Brace L H, Brington H C, Parks A D & Pelz D T, *J Geophys Res (USA)*, **32** (1977) 3183.